REFERENCES

1. Kaplan WB, Zimmerman RE, Bloomer WW, Knapp RC, Adelstein SJ. Therapeutic intraperitoneal ^{32}P: a clinical assessment of the dynamic of distribution. *Radiology* 1981;138:683–688.
2. Tally TE, Goldberg ME, Loken MK. The use of ^{99m}Tc sulfur colloid to assess the distribution of ^{32}P chromic phosphate. *J Nucl Med* 1974;15:190–191.
3. Muller JH. Curative aim and results of routine intraperitoneal radiocolloid administration in treatment of ovarian cancer. *AJR* 1963;89:533–540.
4. Keettel WC, Fox MR, Longnecker DS, et al. Prophylactic use of radioactive gold in the treatment of primary ovarian cancer. *Am J Obstet* 1966;94:766–779.
5. Decker DG, Webb MJ, Holbrook MA. Radiogold treatment of epithelial cancer of the ovary: late Results. *Am J Obstet Gynecol* 1973;115:751–758.
6. Soper JT, Wilkinson RH Jr, Bandy LC, Clarke-Pearson DL, Creasman WT. Intraperitoneal chromic phosphate ^{32}P as salvage therapy for persistant carcinoma of the ovary after surgical restaging. *Am J Obstet Gynecol* 1987;156:1153–1158.
7. Spencer TR Jr, Marks RD Jr, Fenn JO, Jenrette JM 3rd, Lutz MH. Intraperitoneal ^{32}P after negative second-look laparotomy in ovarian carcinoma. *Cancer* 1989;63:2434–2437.
8. Varia M, Rosemam J, Venkatramar S, Askim F, et al. Intraperitoneal chromic phosphate therapy after second-look laparotomy for ovarian cancer. *Cancer* 1988;61:919–927.
9. Reddy S, Sutton GP, Stehmar FB, Hornback NB, Ehrlich CE. Ovarian carcinoma: adjuvant treatment with ^{32}P. *Radiology* 1987;165:275–278.
10. Piver MS, Lele SB, Bakshi S, Parthasarathy KL, Emlich LJ. Five and ten-year estimated survival and disease-free rates after intraperitoneal chromic phosphate, Stage I ovarian adenocarcinoma. *Am J Clin Oncol* 1988;11:515–519.
11. Klaasen D, Shelley W, Starreveld A, et al. Early stage ovarian cancer: a randomized clinical trial comparing whole abdominal radiotherapy, melphalan and intraperitoneal chromic phosphate: a National Cancer Institute of Canada Clinical Trials Group report. *J Clin Oncol* 1988;6:1254–1263.
12. Tulchinsky M, Eggli DF. Intraperitoneal distribution imaging prior to chromic phosphate. Therapy in ovarian cancer patients. *Clin Nucl Med* 1994;19:43–48.
13. Kirsch CM, Chui DW, Yenokida GG, Jensen WA, Bascomb PB. Case report: hepatic hydrothroax with ascites. *Am J Med Sci* 1991;302:103–106.
14. Faiyaz U, Gopal PC. Unilateral pleural effusion without ascites in liver cirrhosis. *Postgrad Med* 1983;74:309–315.
15. Emerson PA, Davies JH. Hydrothorax complicating ascites. *Lancet* 1955;268:487–488.
16. Johnston RF, Loo RV. Hepatic hydrothorax: studies to determine the source of the fluid and report of thirteen cases. *Ann Intern Med* 1969;61:385–401.
17. Lieberman FL, Hidemura R, Peters RL, Reynolds TB. Pathogenesis and treatment of hydrothorax complicating cirrhosis with acites. *Ann Intern Med* 1966;341–351.
18. Rubinstein D, McIness IE, Dudley FJ. Hepatic hydrothorax in the absence of clinical ascites. Diagnosis and management. *Gastroenterology* 1985;88:188–191.
19. Alberts WM, Salem AJ, Solomon DA, Boyce G. Hepatic hydrothorax. Cause and management. *Arch Intern Med* 1991;151:2383–2388.

Intestinal Leakage of Technetium-99m-MDP in Primary Intestinal Lymphangiectasia

Kyung Han Lee, June-Key Chung, Dong Soo Lee, Myung Chul Lee, In Sung Song and Chang-Soon Koh

Departments of Nuclear Medicine and Internal Medicine, Seoul National University Hospital, Seoul, Korea

We present a case in which a patient with primary intestinal lymphangiectasia demonstrated abnormal intestinal accumulation of tracer during ^{99m}Tc-methylene diphosphonate (MDP) skeletal scintigraphy. Early intestinal leakage with gradual colonic migration and concentration was confirmed by repeat bone scan with serial acquisitions. The mechanism for the intestinal localization of ^{99m}Tc-MDP seen in this patient is not clear. Thus, intestinal lymphangiectasia can be a cause for extra-osseous localization of bone scan agents in the intestine.

Key Words: intestinal lymphangiectasia; technetium-99m-MDP

J Nucl Med 1996; 37:639–641

Intestinal lymphangiectasia is characterized by a generalized disorder of the lymphatic channels causing dilated intestinal lymphatics, enteric protein loss, edema, hypoalbuminemia and lymphopenia (*1*). It is usually diagnosed on the basis of a characteristic small bowel mucosal histology along with methods demonstrating enteric protein loss (*2*). We report a patient with primary intestinal lymphangiectasia in whom abnormal intestinal leakage of ^{99m}Tc-methylene diphosphonate was demonstrated unexpectantly during bone scintigraphy.

CASE REPORT

A 23-yr-old woman presented with generalized edema, recurrent tetanic attacks, multiple bone pain, tingling sensation and diarrhea. She had experienced episodes of generalized edema and easy fatigue that had waxed and waned for 2 yr before admission. Physical examination revealed pitting edema of both legs and sclerotic degenerative fingernails. Initial laboratory tests showed severe hypoalbuminemia (15 g/liter), hypocalcemia (total calcium 1.2 mmole/liter; ionized calcium 0.15 mmole/liter), hypokalemia (3.7 mmole/liter), lymphopenia (400/mm^3), increased serum alkaline phosphatase level (316 IU/liter) and an abnormally elevated α_1-antitrypsin clearance rate (249 ml/day). Renal and liver function tests were normal. A small bowel series disclosed diffuse wall thickening of the small intestine, while computed tomography showed no specific abnormalities. Bone scintigraphy with ^{99m}Tc-methylene diphosphonate (MDP) was performed to evaluate multiple bone pain. The bone scan showed diffuse increased skeletal uptake with a focal tibial lesion, poor soft-tissue and renal activity and an unexpected abnormal accumulation of activity in the upper abdomen conforming to the transverse colon (Fig. 1).

The general pattern of tracer distribution that was seen in the patient was compatible with metabolic bone change due to secondary hyperparathyroidism from hypocalcemia, which was attributed to malabsorption. Since the abdominal activity could not be explained, a bone scan was repeated 17 days later with serial images of 30-min intervals. In the repeat bone scan, early images demonstrated diffuse abdominal activity in the small intestinal region. The delayed images confirmed gradual colonic accumulation of the activity (Fig. 2). Lymphoscintigraphy with ^{99m}Tc-antimony colloid disclosed dilated lymphatic channels in the lower extremities and abnormal abdominal tracer activity that later localized in the intestinal region (Fig. 3). The diagnosis of primary intestinal lymphangiectasia was established by clinical findings, laboratory results and pathology from intestinal biopsy (Fig. 4).

DISCUSSION

Primary intestinal lymphangiectasia is a relatively uncommon entity in which congenital central or peripheral lymphatic dysplasia produces functional lymphatic obstruction (*1*). The disease is characterized by dilated intestinal submucosal and subserosal lymphatics, protein losing enteropathy, hypoalbuminemia, hypoproteinemic edema and lymphopenia. Excessive enteric loss of proteins has been shown to be the cause for hypoalbuminemia in this disease (*2*).

In this patient, hypoalbuminemia could be attributed to

Received Feb. 16, 1995; revision accepted Aug. 17, 1995.

For correspondence or reprints contact: Myung Chul Lee, MD, Department of Nuclear Medicine, Seoul National University Hospital, 28 Yungun-dong, Chongno-ku, Seoul 110-744, Korea.

FIGURE 1. Technetium-99m-MDP bone scan at 4 hr postinjection demonstrates diffusely increased axial bone uptake with focal increased activity in the left tibia. Abnormal abdominal activity localized in a curvilinear pattern conforming to the ascending and transverse colon is also shown.

excessive enteric protein loss since the α_1-antitrypsin clearance rate was abnormally elevated (249 ml/day) while there was no evidence of liver dysfunction or proteinuria. Ectatic intestinal lymphatics could be confirmed from pathologic findings. Secondary intestinal lymphangiectasia was unlikely considering the absence of evidence of right heart failure, tuberculosis, cancer, lymphoma, Whipple disease, Celiac disease or lymphadenopathy (*3*). Lymphoscintigraphic agents have been shown to accumulate in the intestine after subcutaneous injection into the feet (*4*). This can be attributed to retrograde lymphatic flow to the intestine, and was demonstrated in intestinal lymphangiectasia with radio-opaque lymphangiography (*5*). Such retrograde intestinal lymphatic flow, with luminal leakage of the radioisotopes, appears to be the explanation for the abnormal bowel accumulation of radioactivity during lymphoscintigraphy in this case.

The mechanism for the observed colonic accumulation of ^{99m}Tc-MDP, however, is less clear. Imaging with labeled albumin can aid in the diagnosis of enteric protein loss by showing intestinal accumulation of radioactivity (*6*). Also, a significant portion of MDP binds to plasma proteins in the early stage. Therefore, it is possible that interstitially extravasated tracer bound proteins are reabsorbed by local lymphatics, moved proximally up to the level of partial obstruction, and then transported retrograde to the intestinal lymphatic system where they are excreted intraluminally via dilated lymphatics. The excreted activity, however, does not need to be in protein-bound form. Unbound ^{99m}Tc-MDP may also have been excreted into the bowel by a similar process.

It therefore appears that enteric loss of ^{99m}Tc-MDP in the small bowel with tracer concentration after distal migration and water absorption in the transverse colon is the mechanism for the unusual localization seen in this patient. This is supported by the findings of early intestinal activity with delayed colonic localization seen in the serial bone scan. Bone scanning agents are known to be detected within the colonic lumen when concen-

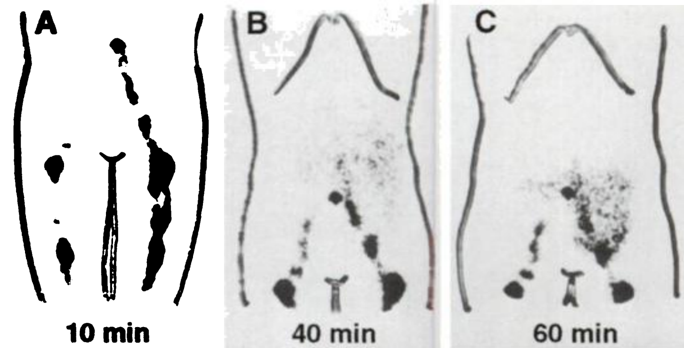

FIGURE 3. (A) Lymphangiography with ^{99m}Tc-antimony colloid subcutaneously injected into the feet showed abnormally dilated iliofemoral lymphatic channels with delayed clearance. There is abnormal diffuse activity in the abdomen at 40 min (B), which is better localized in the intestinal region by 60 min (C).

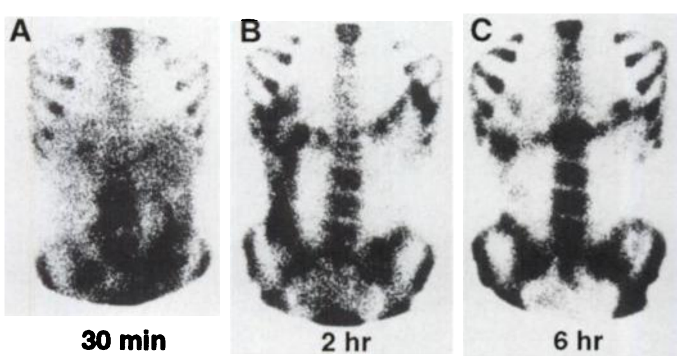

FIGURE 2. A repeat bone scan was obtained with serial images 17 days after the first study, which reconfirmed gradual accumulation radioactivity in the colon. An early image at 30 min after injection showed diffuse midabdominal activity (A), which gradually localized to the ascending and transverse colon by 2 hr (B) and migrated more distally by 6 hr (C).

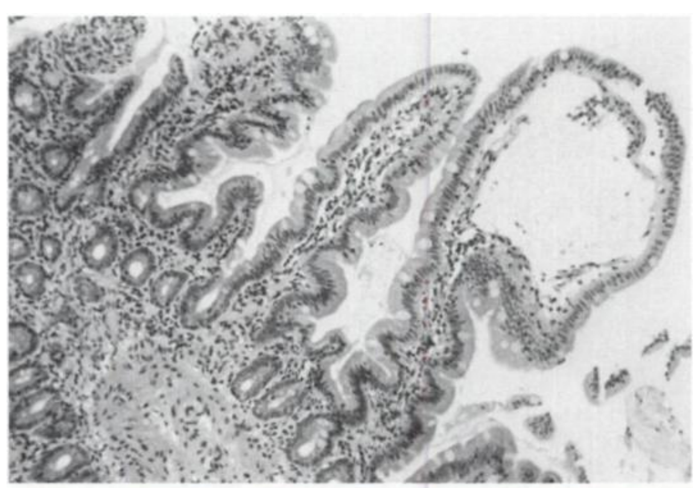

FIGURE 4. Microscopic finding of ileal mucosa biopsy showing blunted villi with ectatic lymphatics in the lamina propria confirmed the diagnosis of intestinal lymphangiectasia (H&E stain 200×).

trated through water absorption (7). Excess biliary excretion due to improper radiopharmaceutical preparation can be excluded as the cause since there was no visualization of the liver in the serial bone scan at any time and other bone scans performed on the same day showed a normal distribution of tracers.

REFERENCES

1. Vardy PA, Lebenthal E, Schwachman H. Intestinal lymphangiectasia: a reappraisal. *Pediatrics* 1975;55:842–851.
2. Puri AS, Aggarwal R, Gupta RK, et al. Intestinal lymphangiectasia: evaluation by CT and scintigraphy. *Gastrointest Radiol* 1992;17:119–121.
3. Fakhri A, Fishman EK, Jones B, Kuhajda F, Siegelman SS. Primary intestinal lymphangiectasia: clinical and CT findings. *J Comp Assist Tomog* 1985;9:767–770.
4. Soucy JP, Eybalin MC, Taillefer R, Levasseur A, Jobin G. Lymphoscintigraphic demonstration of intestinal lymphangiectasia. *Clin Nucl Med* 1983;8:535–537.
5. Mistilis SP, Skyring AP, Stephan DD. Intestinal lymphangiectasia: mechanism of enteric loss of plasma-protein and fat. *Lancet* 1965;1:77–79.
6. Divgi CR, Lisann NM, Yeh SDJ, Benua RS. Technetium-99m-albumin scintigraphy in the diagnosis of protein-losing enteropathy. *J Nucl Med* 1986;27:1710–1712.
7. Conway JJ, Weiss SC, Khentigan A, Tofe AJ, Thane TT. Gallbladder and bowel localization of bone imaging radiopharmaceuticals [Abstract]. *J Nucl Med* 1979;20:622.

Fulminant Hepatic Failure Monitored by Technetium-99m-DTPA-Galactosyl-Human Serum Albumin Scintigraphy

Susumu Shiomi, Tetsuo Kuroki, Masaru Enomoto, Tadashi Ueda, Kyoko Masaki, Naoko Ikeoka, Tadashi Takeda, Kenzo Kobayashi and Hironobu Ochi

Third Department of Internal Medicine and Division of Nuclear Medicine, Osaka City University Medical School, Osaka, Japan

We describe a 43-yr-old woman with fulminant hepatic failure whose progress was monitored scintigraphically using ^{99m}Tc-galactosyl-human serum albumin (^{99m}Tc-GSA). On admission, the liver was atrophic and the heart was delineated distinctly by scintigraphy with ^{99m}Tc-GSA. The receptor index, calculated by dividing the radioactivity of the liver region of interest by the radioactivity of the liver plus heart regions of interest at 15 min post-tracer injection, was very low. As the patient's condition improved, the right lobe of the liver enlarged while the left lobe became atrophic; after 4 mo, the left lobe almost completely disappeared. Delineation of the heart gradually became less distinct, and the receptor index slowly increased. Hepatic receptor imaging with ^{99m}Tc-GSA can define both the hepatic functional reserve and morphological changes of the liver, so it is useful for the diagnosis and follow-up study of fulminant hepatic failure.

Key Words: fulminant hepatic failure; technetium-99m-GSA; hepatic receptor imaging

J Nucl Med 1996; 37:641–643

Technetium-99m-phytate and sulfur colloid, which have been used as liver imaging agents, are transported to the liver and taken up by Kupffer cells after intravenous injection (*1*). The hepatocyte-oriented radiotracer ^{99m}Tc galactosyl-neoglycoalbumin (^{99m}Tc-GSA), developed as a receptor-binding radiopharmaceutical for noninvasive assessment of liver function, is a synthetic radioligand to the asialoglycoprotein receptor (hepatic-binding protein), which resides on the plasma membrane of liver cells. Upon intravenous injection, ^{99m}Tc-GSA is directed to hepatocytes because of its chemical recognition and binding by a specific receptor of hepatic-binding protein. After binding, it is transferred to hepatic lysosomes by receptor-mediated endocytosis (*2,3*).

The use of ^{99m}Tc-GSA enables us not only to evaluate hepatic function in patients with diffuse liver diseases but also to assess morphological changes of the liver. We describe a patient with fulminant hepatic failure who was evaluated scintigraphically with ^{99m}Tc-GSA.

CASE REPORT

A 43-yr-old woman consulted a physician because of general fatigue and clouding of consciousness. The results of clinical tests showed severe liver dysfunction. She was referred to our hospital for further examination and therapy. On admission, physical examination showed jaundice and ascites, and there was clouding of consciousness. Her white blood cell count was 10,100/mm^3, red blood cell count was 362 $\times$ 10^4/mm^3, total bilirubin was 13.2 mg/dl, aspartate aminotransferase was 109 IU/liter, alkaline phosphatase was 372 IU/liter, serum albumin was 2.8 g/dl, lactate dehydrogenase was 512 WU/liter, and the prothrombin time was 25%. Anti-hepatitis A antibody, hepatitis B surface antigen and hepatitis C virus antibody were not detected. Hepatic injury, caused by diclofenac sodium, was diagnosed by results of a lymphocyte stimulation test. On abdominal CT, the liver showed extensive low-density regions and atrophy of both lobes (Fig. 1).

The patient responded to intensive therapy including plasmapheresis. Hepatic receptor imaging with ^{99m}Tc-GSA was performed four times (on admission and after 1, 2 and 4 mo). One 185-MBq dose of ^{99m}Tc-GSA was injected intravenously and dynamic imaging was performed with the patient supine under a large field of view gamma camera with a low-energy, all-purpose parallel-hole collimator. Computer acquisition of the gamma camera data was started just before injection of ^{99m}Tc-GSA and was stopped 20 min later. Digital images (128 $\times$ 128 pixels) were acquired in the byte mode at a rate of 60 sec/frame. Accumulation images of the anterior abdominal view were obtained at 20 min after the injection. Time-activity curves for the heart and liver were generated from regions of interest (ROIs) for the whole liver and precordium. The receptor index (LHL15) was calculated by dividing the radioactivity of the liver ROI by the radioactivity of the liver plus heart ROIs at 15 min after the injection.

Received Mar. 3, 1995; revision accepted Jun. 29, 1995.

For correspondence or reprints contact: Susumu Shiomi, MD, Third Department of Internal Medicine, Osaka City University Medical School, 1-5-7 Asahimachi, Abeno-ku, Osaka 545, Japan.